Anal. Chem. **2007,** *79,* 6690−6696

Electrochemiluminescence Sensors for Scavengers of Hydroxyl Radical Based on Its Annihilation in CdSe Quantum Dots Film/Peroxide System

Hui Jiang and Huangxian Ju*

Key Laboratory of Analytical Chemistry for Life Science (Ministry of Education of China), School of Chemistry and Chemical Engineering, Nanjing University, Nanjing 210093, P. R. China

This work elucidated the detailed electrochemiluminescence (ECL) process of the thioglycolic acid-capped CdSe quantum dots (QDs) film/peroxide aqueous system. The QDs were first electrochemically reduced to form electrons-injected QDs ~ −1.1 V, which then reduced hydrogen peroxide to produce OH• radical. The intermediate OH• radical was a key species for producing holes-injected QDs. The ECL emission with a peak at −1.114 V was demonstrated to come from the $1S_e-1S_h$ transition emission. Using thiol compounds as the model molecules to annihilate the OH• radical, their quenching effects on ECL emission were studied. This effect led to a novel strategy for ECL sensing of the scavengers of hydroxyl radical. The detection results of thiol compounds showed high sensitivity, good precision, and acceptable accuracy, suggesting the promising application of the proposed method for quick detection of both scavengers and generators of hydroxyl radical in different fields.

Well-known, nanoparticle-based biotechnology has attracted special interest in the current development of biosensing application due to the amplification or catalytic effect of the nanostructures and the outstanding optical, electronic, and magnetic performances of functional nanoparticles.[1] Among the miscellaneous functional nanomaterials, quantum dots (QDs) are of considerable interest in bioassays and bioimagings owing to the unique size-dependent optical and electronic properties.[2] The fluoroscent,[3] fluorescence or chemiluminescence resonance energy transfer,[4,5] and electrochemical analytical techniques[6,7] coupled with QDs have been rapidly developed. At the same time, the electrochemiluminescence (ECL) of QDs has also gained particular concern since the ECL of Si QDs was first observed by Bard et al. in 2002.[8] The ECL processes from multifarious QDs, e.g., TOPO-capped CdSe[9] and CdTe QDs,[10] and a CdSe/ZnSe core−shell structure,[11] have been extensively investigated in organic solutions.

Recently, increasing numbers of reports have observed the ECL phenomena of QDs in aqueous media.[12−15] Our previous work observed the enhanced cathodic ECL of CdSe QDs thin film in the aqueous system by using peroxide as coreactant and proposed a method for the detection of H_2O_2.[12] Subsequently, the ECL of CdSe hollow spheres,[13] CdS−carbon nanotube composites[14] in phosphate buffer were also reported. Wang et al.[15] described the ECL of CdO semiconductors at a Pt electrode with peroxydisulfate as the coreactant. Although cadmium chalcogenide nanoparticles have been well accepted as the ECL indicators, no work applies ECL signals of QDs in a sensing purpose besides the detections of peroxide[12] and glucose[16] suggested by our group. To further develop the ECL applications of QDs by use of the interaction between analytes and the species involved in the ECL process, it is necessary to understand the intermediates generated in the ECL system. This work elucidated the cathodic ECL process of the CdSe QDs thin film in the presence of hydrogen peroxide as a coreactant. The hydroxyl radical, which was produced from the reduction of hydrogen peroxide by electrons-injected QDs, was demonstrated to be a key intermediate for producing holes-injected QDs and thus the ECL emission. The quenching effects of radical scavengers, using thiol compounds as the model molecules, on the ECL were also observed. Therefore, a novel ECL sensor for thiol compounds was proposed.

* Corresponding author. Phone: +86-25-83593593. Fax: +86-25-83593593. E-mail: hxju@nju.edu.cn.

(1) Wang, J. *Small* **2005**, *1*, 1036−1043.
(2) Michalet, X.; Pinaud, F. F.; Bentolila, L. A.; Tsay, J. M.; Doose, S.; Li, J. J.; Sundaresan, G.; Wu, A. M.; Gambhir, S. S.; Weiss, S. *Science* **2005**, *307*, 538−544.
(3) Goldman, E. R.; Clapp, A. R.; Anderson, G. P.; Uyeda, H. T.; Mauro, J. M.; Medintz, I. L.; Mattoussi, H. *Anal. Chem.* **2004**, *76*, 684−688.
(4) Goldman, E. R.; Medintz, I. L.; Whitley, J. L.; Hayhurst, A.; Clapp, A. R.; Uyeda, H. T.; Deschamps, J. R.; Lassman, M. E.; Mattoussi, H. *J. Am. Chem. Soc.* **2005**, *127*, 6744−6751.
(5) Huang, X. Y.; Li, L.; Qian, H. F.; Dong, C. Q.; Ren, J. C. *Angew. Chem., Int. Ed.* **2006**, *45*, 5140−5143.
(6) Liu, G.; Wang, J.; Kim, J.; Jan, M. R.; Collins, G. E. *Anal. Chem.* **2004**, *76*, 7126−7130.
(7) Hansen, J. A.; Wang, J.; Kawde, A.; Xiang, Y.; Gothelf, K. V.; Collins, G. *J. Am. Chem. Soc.* **2006**, *128*, 2228−2229.
(8) Ding, Z.; Quinn, B. M.; Haram, S. K.; Pell, L. E.; Korgel, B. A.; Bard, A. J. *Science* **2002**, *296*, 1293−1297.
(9) Myung, N.; Ding, Z.; Bard, A. J. *Nano Lett.* **2002**, *2*, 1315−1319.
(10) Bae, Y.; Myung, N.; Bard, A. J. *Nano Lett.* **2004**, *4*, 1153−1161.
(11) Myung, N.; Bae, Y.; Bard, A. J. *Nano Lett.* **2003**, *3*, 1053−1055.
(12) Zou, G. Z.; Ju, H. X. *Anal. Chem.* **2004**, *76*, 6871−6876.
(13) Zou, G. Z.; Ju, H. X.; Ding, W. P.; Chen, H. Y. *J. Electroanal. Chem.* **2005**, *579*, 175−180.
(14) Ding, S. N.; Xu, J. J.; Chen, H. Y. *Chem. Commun.* **2006**, 3631−3633.
(15) Kang, J. Z.; Wei, H.; Guo, W. W.; Wang, E. K. *Electrochem. Commun.* **2007**, *9*, 465−468.
(16) Jiang, H.; Ju, H. X. *Chem. Commun.* **2007**, 404−406.

10.1021/ac071061j CCC: $37.00
Published on Web 08/04/2007

Small peptides and amino acids with sulfydryl groups, such as glutathione (γ-L-glutamyl-L-cysteine-glycine, GSH) and L-cysteine, play essential roles in life processes.[17] The abundant GSH in the tissues and cells normally acts as the main antioxidant to regulate the physiological environment. Its level is related to diabetes and some cancers.[18] L-Cysteine is also involved in a variety of important cellular functions including protein synthesis, detoxicfication, and metabolism, and its insufficiency may cause many diseases.[19] Thus, the determination of both GSH and L-cysteine levels is of great significance. Several techniques have been reported for their analyses, including spectrophotometry,[20] fluorometry,[21,22] electrochemistry,[23,24] chemiluminescence (CL),[25,26] and ECL.[27] Compared with the ECL method based on the tris(2,2′-bipyridine)ruthenium(II) system,[27] the proposed strategy was nonconsumable and carried out the detection of GSH and L-cysteine at negative potential, and thus excluded the interference from some important biological species such as other amino acids and 3-substituted indole derivatives.

The detection results of model molecules show the applicable feasibility of the strategy for detection of all the analytes that can scavenge or generate the radical intermediate, including the compounds in biological, environmental, food, industrial, medical, and energy source fields. Thus, the proposed method and ECL sensor could be further developed in different fields for analytical purposes, which would be helpful in development of quantum dots materials and their practical applications.

EXPERIMENTAL SECTION

Reagents. GSH and its oxidized form (GSSG), L-cysteine, L-cystine, thioglycolic acid (TGA), and 5,5-dimethylpyrrolidine-*N*-oxide (DMPO) were purchased from Sigma-Aldrich (St. Louis, MO). All reagents were used as received. The 0.1 M phosphate buffer solution containing 0.1 M KNO_3 (PBS) was used throughout this work, and the buffer pH was adjusted by changing the ratio of Na_2HPO_4 to NaH_2PO_4. Double-distilled water was used throughout.

The paraffin-impregnated graphite electrode (PIGE, 3.0-mm radius) was prepared according to ref 12, polished successively on abrasive papers of 800 and 4000 mesh to obtain a smooth surface, and then rinsed thoroughly with water. Before use, the electrode was electrochemically pretreated at an applied potential of +1.75 V for 10 min in 0.1 M pH 5.0 PBS, followed with ultrasonication and rinsing in water, to enhance the surface hydrophilicity.[28]

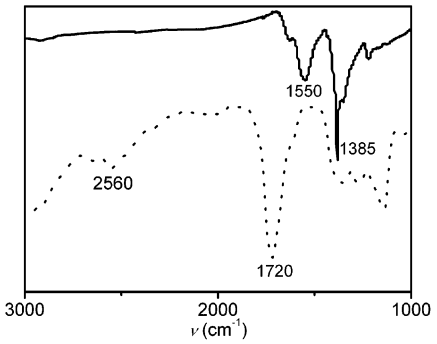

Figure 1. FT-IR spectra of TGA (dotted line) and TGA-capped CdSe QDs (solid line).

Apparatus. ECL was conducted on a CHI 812 electrochemical working station (CHI Co.,) with a homemade ECL system comprising a CdSe/TGA QDs film modified working electrode, a Pt counter electrode, and a Ag/AgCl (saturated KCl) reference electrode. The ECL emission was detected synchronously with a luminescence analyzer (IFFM-D, Remax Electronic Instrument Limited Co., Xi'an, China) at room temperature. The observation window was placed in front of the photomultiplier tube (detection range from 300 to 650 nm) biased at −800 V. UV−vis absorption spectra were acquired with a Perkin-Elmer photospectrometer (Perkin-Elmer Co.). The FT-IR spectra were recorded with a Vector 22 FT-IR spectrometer (Bruker Co.). Scanning electron micrographs (SEM) of different films were obtained with a LEO 1530 VP scanning electron microscope (Leo Ltd.), equipped with an Inca 300 EDS (Oxford Ltd.). Both ECL and photoluminescence (PL) spectra were taken on a Jasco 820 FP fluorometer (Jasco Co.). Electron paramagnetic resonance (EPR) spectra were recorded on an EMX-10/12 EPR spectrometer (Bruker Co.).

Syntheses and Characterization of TGA-Capped CdSe (CdSe/TGA) QDs. CdSe/TGA QDs were synthesized using a slightly modified procedure reported previously.[29] After 20 mL of 5 mM $CdCl_2$ was mixed with 20 μL of TGA; 1 M NaOH was added to adjust its pH to 11.2. The clear solution was diluted to 50 mL and bubbled with highly pure N_2 for 30 min. Then 0.5 mL of 0.1 M Na_2SeSO_3 was injected into this mixture to obtain a clear light yellow solution of CdSe/TGA QDs. The final molar ratio of Cd^{2+}/TGA/Se^{2-} was ∼1:2.5:0.5. The sizes of the obtained QDs could be tuned by simply varying the reflux time. The QDs solution was then dialyzed against water for 48 h and centrifuged to remove a morsel of precipitate. The final solution could be rather stable for 2 months when stored in a refrigerator at 4 °C.

Precaution! The cadmium salts should be handled with care due to their toxicity and environmental hazard.

The FT-IR spectrum of TGA showed a peak at 2560 cm^{-1} for stretch vibration of the S−H bond, which diminished in the spectrum of 2.5-nm CdSe/TGA QDs (Figure 1), indicating the formation of S−Cd bonds between TGA and CdSe core. These spectra showed a shift of the asymmetric vibration of the carboxyl group in TGA from 1720 to 1550 cm^{-1}, implying that the COOH in TGA turned to its anion, which also led to the appearance of the symmetric vibration of the carboxyl anion at 1385 cm^{-1}. In

(17) Meister, A.; Anderson, M. E. *Annu. Rev. Biochem.* **1983**, *52*, 711−760.
(18) Curello, S.; Ceconi, C.; Cargnoni, A.; Cornacchiari, A.; Ferrari, R.; Albertini, A. *Clin. Chem.* **1987**, *33*, 1448−1449.
(19) Kleinman, W. A.; Richie, J. P. *Biochem. Pharmacol.* **2000**, *60*, 19−29.
(20) Pastore, A.; Federici, G.; Bertini, E.; Piemonte, F. *Clin. Chim. Acta* **2003**, *333*, 19−39.
(21) Chen, S. J.; Chang, H. T. *Anal. Chem.* **2004**, *76*, 3727−3734.
(22) Kawakami, S. K.; Gledhill, M.; Achterberg, E. P. *TrAC-Trends Anal. Chem.* **2006**, *25*, 133−142.
(23) Liu, J. F.; Roussel, C.; Lagger, G.; Tacchini, P.; Girault, H. H. *Anal. Chem.* **2005**, *77*, 7687−7694.
(24) Inoue, T.; Kirchhoff, J. R. *Anal. Chem.* **2000**, *72*, 5755−5760.
(25) Wang, S. J.; Ma, H. M.; Li, J.; Chen, X. Q.; Bao, Z. J.; Sun, S. N. *Talanta* **2006**, *70*, 518−521.
(26) Lau, C.; Qin, X.; Liang, J.; Lu, J. *Anal. Chim. Acta* **2004**, *514*, 45−49.
(27) Chen, G. N.; Jian, W.; Xi, C.; Duan, J. P.; Zhao, Z. F.; Chen, H. Q. *Analyst* **2000**, *125*, 2294−2298.
(28) Wang, H. S.; Ju, H. X.; Chen, H. Y. *Electroanalysis* **2001**, *13*, 1105−1109.
(29) Gaponik, N.; Talapin, D. V.; Rogach, A. L.; Hoppe, K.; Shevchenko, E. V.; Kornowski, A.; Eychmüller, A.; Weller, H. *J. Phys. Chem. B* **2002**, *106*, 7177−7185.

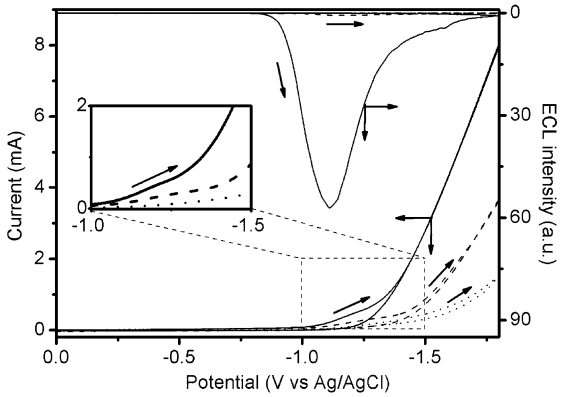

Figure 2. Cyclic voltammograms and ECL curves at QDs film modified PIGE in deaerated 0.1 M pH 9.3 PBS in the absence (dash line) and presence (solid line) of 300 μM H_2O_2 and the bare electrode in deaerated 0.1 M pH 9.3 PBS containing 300 μM H_2O_2 (dotted line) as control. Scan rate, 100 mV s^{-1}. Inset, amplification of cathodic waves from −1.0 to −1.5 V.

total, the structure of the obtained QDs could be identified as a cadmium-rich CdSe core covered with excess TGA^{2-} anions.[30]

Preparation of QDs Film. The 15 μL of QDs solution was cast on the pretreated PIGE to form the even QDs film. After being dried in air at 4 °C, the formed film was washed twice with double-distilled water and stored in 0.1 M pH 7.0 PBS at 4 °C. This film was stable due to the strong physical adsorption of QDs on the surface of the PIGE. For characterization, QDs samples were deposited on the PIGE substrates with similar steps for SEM measurements.

RESULTS AND DISCUSSION

ECL Behavior and Morphology of QDs Film. Here, TGA-capped CdSe QDs were selected as the ECL emitter. At the QDs (with an estimated size of 2.5 nm) film modified PIGE immersed in a deaerated 0.1 M pH 9.3 PBS containing 300 μM H_2O_2, a strong cathodic ECL signal could be observed at about −1.114 V accompanied with a tiny shoulder peak around −1.578 V (Figure 2). The control experiments showed that both the QDs film and the presence of peroxide in the deaerated solution were imperative for obtaining the intensive ECL signal. When a low amount of QDs were evenly dispersed on the electrode surface, the shoulder disappeared due to the absence of interaction with each other, suggesting the shoulder peak was identified as the emission of the luminophores from QDs assemblies.[12] The sharp ECL could be considered as the emission from excited states of QDs generated in the reaction of peroxide and reduced individual CdSe nanocrystal species during the cathodic scan. This ECL peak was the focus in the following research.

The morphologies of QDs films were observed with SEM, which showed that the coating of 2.5-nm CdSe/TGA QDs on the PIGE produced a layer of QDs film with the aggregate size less than 20 nm (Figure 3). This size range was much smaller than those of 50−300 nm for unmodified CdSe QDs,[12] probably due to the electrostatic repulsion among these negatively charged caps (TGA^{2-}) around CdSe cores. The decline in aggregation was favorable for improving the ECL efficiency. The density of these

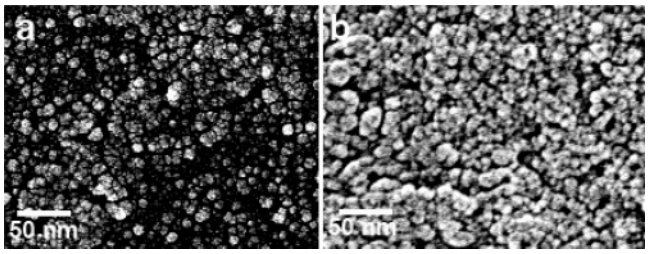

Figure 3. SEM images of QDs films formed with (a) 5 and (b) 15 μL of 0.021 mM TGA-capped CdSe (2.5 nm) on the PIGE substrates.

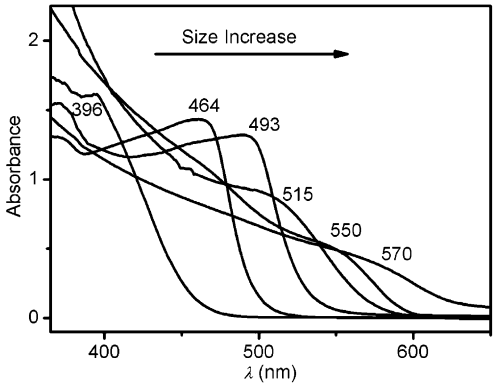

Figure 4. UV−vis spectra of a series of QDs obtained after dialysis and 1:1 dilution with water.

Table 1. Size Effect on ECL Intensity and Peak Potential

λ (nm)	band gap (eV)	*d* (nm)	concn (mM)	ECL intensity (norm.)	ECL peak potential (V *vs* Ag/AgCl)	norm. ratio[a]
396	3.14	1.5	0.18	0.16	−1.59	0.019
464	2.68	2.0	0.072	3.90	−1.51	1.14
493	2.52	2.3	0.050	13.1	−1.40	5.50
515	2.41	2.5	0.021	100	−1.11	100
550	2.26	3.0	0.009	25.5	−1.03	59.5
570	2.18	3.5	0.005	2.77	−1.03	11.6

[a]Normalized ratio of ECL intensity to surface concentration of QDs.

aggregates depended on the amount of QDs solution used for coating. The QDs film formed with 15 μL of solution (Figure 3b) was much denser than that formed with 5 μL of solution (Figure 3a), and in the optimization steps, the former film showed greater ECL response to H_2O_2.

Size Effect of QDs on the ECL. The sizes and concentrations of QDs, estimated from the wavelength of the first absorption peak in UV−vis spectra (Figure 4), according to the empirical equations,[31] are listed in Table 1. The size of the QDs could be observed to deeply affect the ECL peak potential and intensity. The ECL peak potential shifted positively with the increasing size or the decreasing band gap of the QDs, indicating that the injection of electrons to the surface states of smaller QD particles should be more difficult. A similar relationship between the band gap of CdTe QDs and their electrochemical behaviors was also observed.[32] The ECL peak intensity increased with the decreasing band gaps, i.e., the increasing sizes, even if the surface concentra-

(30) Gao, M. Y.; Richter, B.; Kirstein, S. *Adv. Mater.* **1997**, *9*, 802−805.

(31) Yu, W. W.; Qu, L. H.; Guo, W. Z.; Peng, X. G. *Chem. Mater.* **2003**, *15*, 2854−2860.

tion of the QDs was decreasing. However, when the nanoparticles were larger than 2.5 nm, both the ECL intensity and the normalized ratio of ECL intensity to surface concentration of QDs decreased quickly with the increasing QDs size due to the relatively small surface-to-volume ratio of QDs, which also decreased the contact area of QDs with the electrode and thus the efficient electron transfer. The QDs of 2.5 nm gave the most sensitive response and were thus selected as the ECL emitter in this study.

Elucidation of the ECL Mechanism. In the previous work,[12] a concise reaction between electrochemically reduced QDs and peroxide was given to explain the production of excited QDs during the cathodic scan. But the species involved in this process was unclear. As shown in Figure 2, the QDs immobilized at PIGE could be reduced in oxygen-free pH 9.3 PBS to produce a cathodic wave starting at −1.008 V with a peak at −1.247 V, while the reduction of H_2O_2 at bare PIGE started at a more negative potential with much lower current. After H_2O_2 was added into the oxygen-free pH 9.3 PBS, the reduction current of the immobilized QDs increased and the starting potential of the cathodic wave shifted to −0.966 V with a peak around −1.195 V, going with a strong ECL emission with a peak value at −1.114 V, at which the reduction current of the QDs was 3.2 times that in the absence of H_2O_2. The increase in cathodic current and the positive shift of reduction potential indicated the electrocatalysis of the QDs toward the reduction of H_2O_2. Therefore, upon a cathodic scan, CdSe/TGA QDs were first injected with the electrons from the electrode:

$$\mathrm{CdSe/TGA} + \mathrm{e^-} \rightarrow \mathrm{CdSe}(\mathrm{e^-}_{1Se})/\mathrm{TGA} \qquad (1)$$

The electrons-injected QDs then reduced hydrogen peroxide with a simulated Weiss reaction[33] to produce OH• radical:[34]

$$\mathrm{CdSe}(\mathrm{e^-}_{1Se})/\mathrm{TGA} + \mathrm{H_2O_2} \rightarrow \mathrm{CdSe/TGA} + \mathrm{OH^\bullet} + \mathrm{OH^-} \qquad (2)$$

To verify the formation of intermediate OH• at the modified PIGE, EPR spectra were used to record the process in tandem. Before the electrochemical process, the deaerated pH 9.3 PBS containing 300 μM H_2O_2 and 50 mM DMPO as a radical trapper showed three weak signals at 3460, 3475, and 3490 G (curve a in Figure 5A), which were the intrinsic properties of the free DMPO trapper. After immersing the QDs film modified electrode in the same solution and applying a potential of −1.8 V for 150 s, the former three EPR signals significantly attenuated (curve b in Figure 5A), indicating the consumption of the DMPO trapper, while four sharp superfine split peaks with an intensity ratio of 1:2:2:1 appeared, which entirely corresponded with the characteristics of the DMPO−OH adducts,[35] verifying the presence of hydroxyl radical in the system. Thus, the electrochemical process followed by a chemical reaction with H_2O_2 at the QDs film modified electrode in H_2O_2 solution did produce hydroxyl radical.

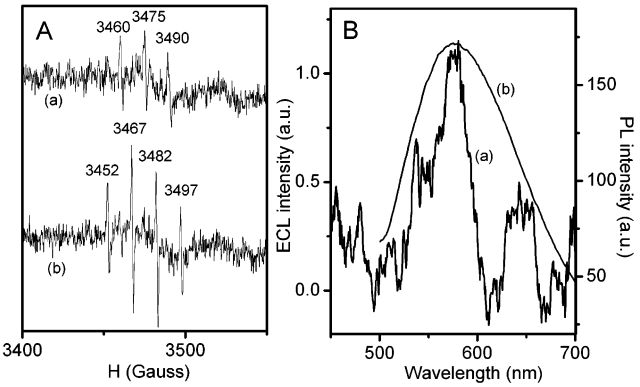

Figure 5. (A) EPR spectra of pH 9.3 PBS containing 300 μM H_2O_2 and 50 mM DMPO recorded before (a) and after (b) the electrochemical process with QDs film modified PIGE at −1.8 V for 150 s. The EPR signal was obtained with an accumulation of five cycles. (B) ECL spectrum of the QDs−H_2O_2 system at a constant potential of −1.8 V obtained with an accumulation of five fast scan (50 nm s^{-1}) from 450 to 700 nm (a) and PL spectrum of the film (b).

The formed OH• radical could then easily inject a hole in the $1S_h$ quantum-confined orbital of the CdSe core (eq 3) due to the high standard redox potential (~2.84−0.06 pH V vs SHE) of OH•/OH^- couple:[34]

$$\mathrm{OH^\bullet} + \mathrm{CdSe/TGA} \rightarrow \mathrm{OH^-} + \mathrm{CdSe}(\mathrm{h^+}_{1Sh})/\mathrm{TGA} \qquad (3)$$

The recombination of the injected holes (h^+) and the injected electrons (e^-) resulted in the formation of excited-state QDs (CdSe/TGA*):

$$\mathrm{CdSe}(\mathrm{e^-}_{1Se})/\mathrm{TGA} + \mathrm{CdSe}(\mathrm{h^+}_{1Sh})/\mathrm{TGA} \rightarrow \mathrm{CdSe/TGA^*} \qquad (4)$$

Simultaneously, injection of a hole into the $\mathrm{CdSe}(\mathrm{e^-}_{1Se})/\mathrm{TGA}$ might also exist:

$$\mathrm{CdSe}(\mathrm{e^-}_{1Se})/\mathrm{TGA} + \mathrm{OH^\bullet} \rightarrow \mathrm{OH^-} + \mathrm{CdSe/TGA^*} \qquad (3a)$$

Both injection processes led to the same luminophore CdSe/TGA*, which then produced light emission:

$$\mathrm{CdSe/TGA^*} \rightarrow \mathrm{CdSe/TGA} + h\nu \qquad (5)$$

The light emission process could be supported by its ECL spectrum. As shown in Figure 5B, the ECL emission located at ~570 nm coincident with the peak position of the PL, indicating that the excited state in the ECL emission was the same as that in the PL, in which the CdSe/TGA* could be considered as the emitter to produce $1S_e-1S_h$ transition emission. This result was different from the mechanism of the surface state-dependent process for the QDs dispersed in the organic systems.[8−11] Another observed weaker emission around 650 nm could be attributed to the trapped emission, as observed in the ECL spectrum of diamines cross-linked 2.8-nm CdSe.[34]

Quenching of ECL Emission. Based on the above comprehension, OH• radical had a key role in the ECL pathways. Either eqs 3 and 4 or 3a indicated that the excited CdSe/TGA* was

(32) Poznyak, S. K.; Osipovich, N. P.; Shavel, A.; Talapin, D. V.; Gao, M. Y.; Eychmuller, A.; Gaponik, N. *J. Phys. Chem. B* **2005**, *109*, 1094−1100.
(33) Weiss, J. *Adv. Catal.* **1952**, *4*, 343−364.
(34) Poznyak, S. K.; Talapin, D. V.; Shevchenko, E. V.; Weller, H. *Nano Lett.* **2004**, *4*, 693−698.
(35) Tabner, B. J.; Turnbull, S.; El-Agnaf, O. M. A.; Allsop, D. *Free Radical Biol. Med.* **2002**, *32*, 1076−1083.

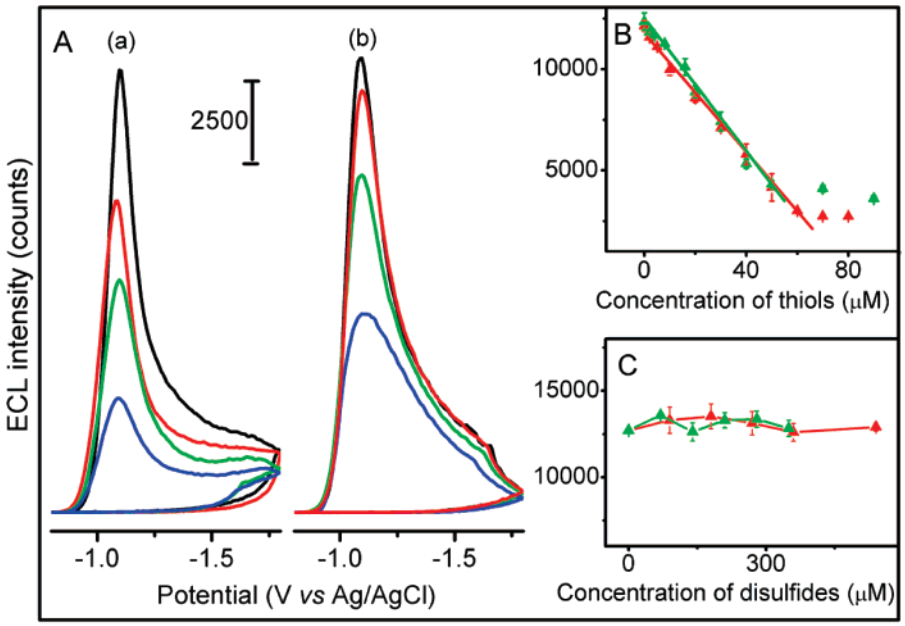

Figure 6. (A) Quenching effects of (a) GSH at 0 (black), 20 (red), 40 (green), and 60 μM (blue) and (b) L-cysteine at 0 (black), 8 (red), 20 (green), and 40 μM (blue) on the ECL. (B) Linear plots of ECL intensity vs GSH (red) and L-cysteine (green) concentrations. (C) Effect of GSSG (red) and L-cystine (green) on the ECL system.

Scheme 1. ECL and Quenching Processes at QDs Film Modified PIGE

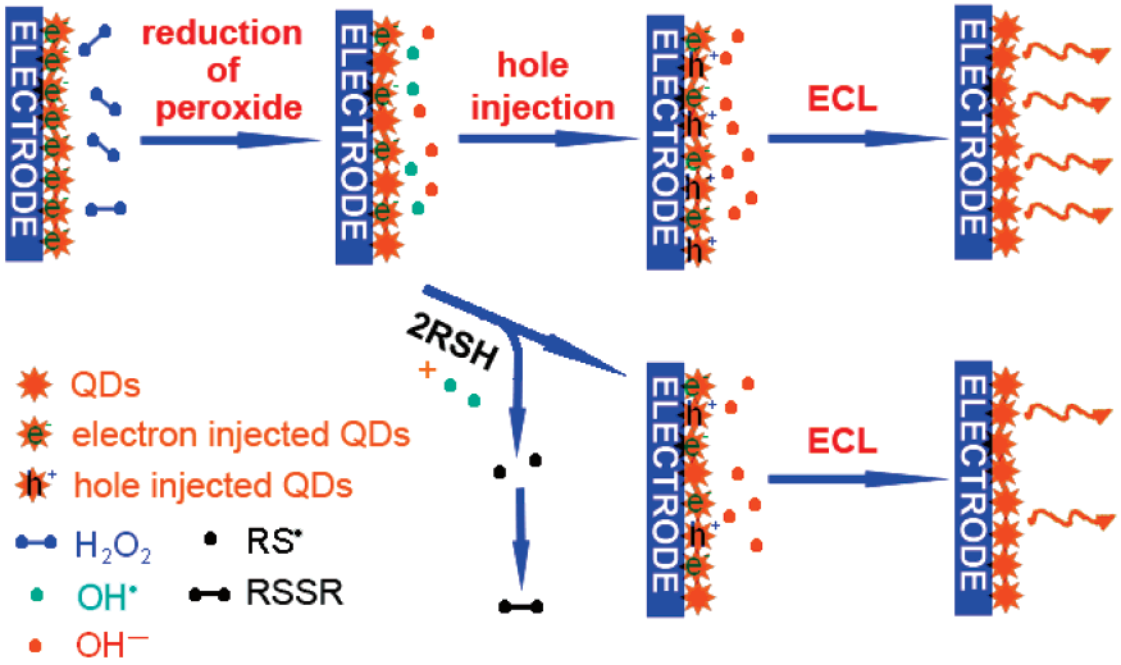

proportional to the amount of hydroxyl radical. Thus, any reaction involved OH• radical would affect the ECL emission. As existed in the biological conditions, thiol compounds could be efficiently oxidized by OH• with the high rate constants between 10^9 and 3×10^{10} mol^{-1} dm^3 s^{-1}.[36] Using these known OH• radical scavengers as models, their quenching effects on the ECL emission are shown in Figure 6A. Upon addition of GSH or L-cysteine to the PBS containing H_2O_2, the ECL intensity at the QDs film modified PIGE decreased greatly, while in the control experiments, GSSG or L-cystine could hardly affect the ECL signals, even at concentrations 10 times that of GSH or L-cysteine (Figure 6C). Furthermore, the ECL intensity upon the cyclic sweep for several cycles was identical, indicating that the sulfydryl group was responsible for the quenching effect according to the following reaction:[36]

$$OH^{\bullet} + RSH \rightarrow RS^{\bullet} + H_2O \quad (6)$$

$$RS^{\bullet} + RS^{\bullet} \rightarrow RS{-}SR \quad (7)$$

The whole ECL process including the quenching effect is shown

(36) Enescu, M.; Cardey, B. *Chem. Phys. Chem* **2006**, *7*, 912−919.

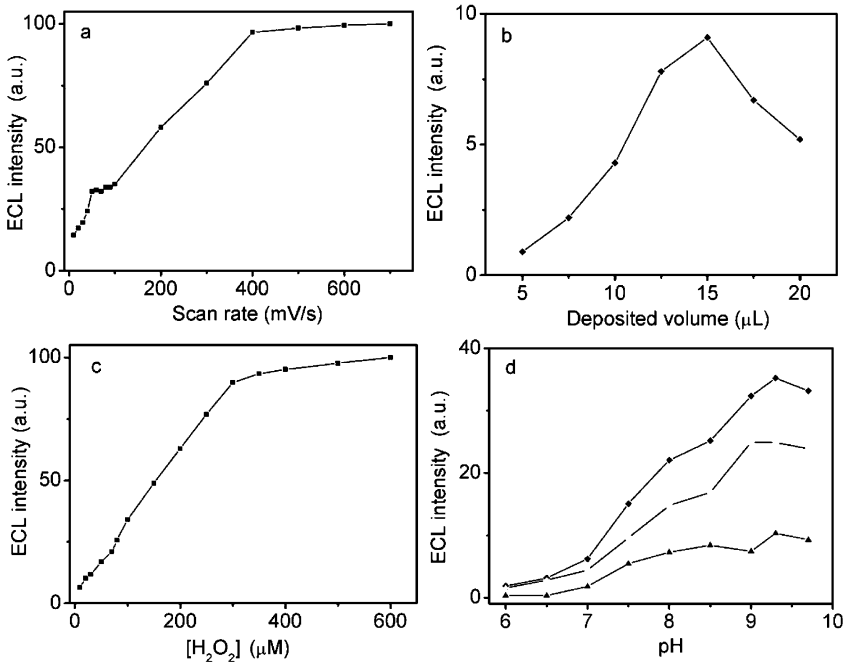

Figure 7. Optimization of relative parameters: (a) scan rate; (b) cast volume of 0.021 mM QDs; (c) H_2O_2 concentration and (d) pH of detection solution. All other factors are at their optimal values during optimizing one parameter. In (d), all the ECL signals were detected in the absence (solid diamonds) and presence (hollow diamonds) of 20 μM GSH, and their differences (solid triangles) are presented to illustrate the criterion of pH selection.

in Scheme 1. Although the stabilizer TGA was also a thiol compound, FT-IR spectra (Figure 1) indicated only S−Cd bonds without an SH group present in the QDs. Thus, it did not quench the ECL emission and interfere with the detection of thiol compounds.

Conditions Optimization. To apply the functional film in chemical and biosensing for the scavengers of radical intermediates, several experimental parameters including potential scan rate, the amount of QDs deposited, solution pH, and the concentration of peroxide were optimized. The scan rate could affect the ECL over a wide range, since the ECL efficiency significantly depended on the rate of generation/annihilation of the excited state (CdSe/TGA)*. At high scan rate, the excited state (CdSe/TGA)* could be enriched in a short time span and thus led to the enhanced ECL intensity (Figure 7A). With the increasing scan rate, the ECL intensity increased and tended to a constant value at the scan rate of 400 mV s^{-1}, indicating the emitted photons came to saturation.

The quantity of (CdSe/TGA)* essentially depended on the deposition amount of the QDs. With an increasing QDs density, the formed individual nanocrystal species in the electrochemical scanning process increased, leading to the enhancement in ECL intensity (Figure 7B). The strongest ECL intensity was obtained at the modified PIGE prepared with 15 μL of CdSe/TGA solution, which corresponded with the close-packed structure of QDs observed in the SEM image (Figure 3). When the volume exceeded 15 μL, the ECL intensity decreased, which indicated that the overloaded QDs could increase the thickness of the film and inhibit the fast electron exchange with the radical species.

As shown in Figure 7C, the increasing concentration of H_2O_2 could steeply enhance the ECL signal until a plateau occurred at 300 μM, at which point the system could provide remarkable sensitivity to the ECL quenching. The quenching response to 20 μM GSH increased with increasing pH until a maximum difference occurred at pH 9.3 (Figure 7D). In summary the ECL intensity for analytical purposes could be detected with a QDs film modified electrode prepared with 15 μL of CdSe/TGA solution at 400 mV s^{-1} in pH 9.3 PBS containing 300 μM H_2O_2.

Thiols Detection Assay. The ECL intensity decreased linearly in the concentration ranges of 2.0−60 μM for GSH ($R = 0.998$) and 2.0−50 μM for L-cysteine ($R = 0.996$) with detection limits of 1.0 μM for GSH and 2.0 μM for L-cysteine at a S/N ratio of 3, respectively (Figure 6B). The LOD of GSH was lower than those of carbon nanotube-based[37] and GSH peroxidase-based amperometric sensors[38] or capacitance sensor with molecularly imprinted technique.[39] The LOD of L-cysteine was also lower than several sensors fabricated with carbon nanostructures.[40,41] Twelve measurements of ECL emission upon continuous cyclic scan in pH 9.3 PBS containing 300 μM H_2O_2 and 40 μM glutathione showed coincident signals with a relative standard deviation (RSD) of 2.7% (Figure 8), indicating the reliability and stability of the signals. The RSDs of five parallel measurements (intraassay) at 40 μM GSH and 40 μM L-cysteine with one QDs film modified electrode were 3.8 and 2.3%, respectively, indicating a good precision. The detection of 40 μM GSH and 40 μM L-cysteine with six electrodes fabricated independently (interassay) showed the RSDs of 5.5 and 6.1%, respectively, giving an acceptable fabricated reproducibility of the QDs films modified electrode. After the QDs modified electrode was stored at 4 °C for 1 month, the ECL intensity for

(37) Chen, G.; Zhang, L. Y.; Wang, J. *Talanta* **2004**, *64*, 1018−1023.
(38) Rover, L.; Kubota, L. T.; Hoehr, N. F. *Clin. Chim. Acta* **2001**, *308*, 55−67.
(39) Yang, L.; Wei, W.; Xia, J.; Tao, H.; Yang, P. *Electroanalysis* **2005**, *17*, 969−977.
(40) Nekrassova, O.; Lawrence, N. S.; Compton, R. G. *Electroanalysis* **2003**, *15*, 1655−1660.
(41) Salimi, A.; Hallaj, R. *Talanta* **2005**, *66*, 967−975.

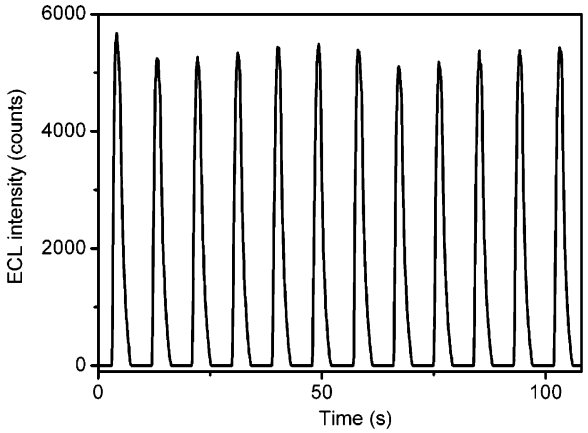

Figure 8. Continuous cyclic scan of QDs film modified PIGE in pH 9.3 PBS containing 300 μM H_2O_2 and 40 μM glutathione.

detection of 20 μM GSH decreased by 4.6%, showing acceptable storage stability.

The effects of foreign species on thiol determination with this ECL sensor were examined. The saline ions in the buffer solution (Na^+, K^+, NO_3^-, and phosphate) did not affect the ECL intensity at concentrations lower than 0.1 M. The mild oxidants, such as $[Fe(CN)_6]^{3-}$ and oxalate, hardly reacted with the thiol groups and showed little influence. Other common amino acids, i.e., tyrosine, glycine, leucine, and 3-substituted indole derivatives were inert to the radical processes, and their interference could be excluded. Dopamine with a concentration beyond 0.1 mM could quench the radicals and interfere with the detection. However, its interference with detection of analytes in the following serum samples was neglectable due to the low level of dopamine in this system.

The concentrations of GSH spiked in serum samples were also detected with the suggested method and the standard Ellman method[20] to examine the accuracy of the proposed method. The results are listed in Table 2. The relative deviations of less than 8% showed the fine accuracy.

Table 2. GSH Detection in Spiked Serum Samples

no.	Ellman method (μM)	proposed method (μM)	RD (%)
1	15.4 ± 0.4	14.2 ± 1.3	−7.8
2	24.3 ± 0.4	24.8 ± 0.3	2.1
3	19.0 ± 0.9	17.7 ± 1.7	−6.8
4	32.5 ± 1.0	34.0 ± 1.2	4.6
5	38.8 ± 1.2	40.9 ± 0.4	5.4

CONCLUSIONS

This work elucidates the ECL process of the CdSe/TGA QDs film modified electrode in aqueous system containing H_2O_2 as coreactant. The ECL arises from the $1S_e-1S_h$ transition emission. The intermediate $OH^\bullet$ radical is a key species in the ECL process. Thus, all $OH^\bullet$ radical involved reactions will quench the ECL emission, producing a novel ECL sensor and a nonconsumable method for analytical purposes, which have been used for detection of thiol compounds with good precision and acceptable accuracy. Furthermore, some important biological species do not interfere with the detection. By combining separation techniques, the proposed method could be used for simultaneous detection of both scavengers and generators of hydroxyl radical in different fields, including clinical testing and drug screening.

ACKNOWLEDGMENT

We gratefully acknowledge the support of the National Science Fund for Distinguished Young Scholars to H.J. (20325518) and Creative Research Groups (20521503), the Key Program from the National Natural Science Foundation of China (20535010) and Postdoctoral Fund from Jiangsu Planned Projects for Postdoctoral Research Funds.

Received for review May 22, 2007. Accepted July 3, 2007.

AC071061J